www.czasopisma.pan.pl PAN POLSKA AKADEMIA NAUK www.journals.pan.pl

Arch. Min. Sci. **67** (2022), 2, 333-354

Electronic version (in color) of this paper is available: http://mining.archives.pl

DOI: https://doi.org/10.24425/ams.2022.141462

PHU MINH VUONG NGUYEN[1*], SYLWESTER RAJWA[1], MAREK PŁONKA[1], WALDEMAR STACHURA[2]

GEOMECHANICAL ASSESSMENTS OF LONGWALL WORKING STABILITY – A CASE STUDY

The stability of longwall mining is one of the most important and the most difficult aspects of underground coal mining. The loss of longwall stability can threaten lives, disrupt the continuity of the mining operations, and it requires significant materials and labour costs associated with replacing the damages. In fact, longwall mining stability is affected by many factors combined. Each case of longwall mining has its own unique and complex geological and mining conditions. Therefore, any case study of longwall stability requires an individual analysis.

In Poland, longwall mining has been applied in underground coal mining for years. The stability of the longwall working is often examined using an empirical method. A regular longwall mining panel (F3) operation was designed and conducted at the Borynia-Zofiówka-Jastrzębie (BZJ) coal mine. During its advancement, roof failures were observed, causing a stoppage. This paper aims to identify and determine the mechanisms of these failures that occurred in the F3 longwall. A numerical model was performed using the finite difference method - code FLAC2D, representing the exact geological and mining conditions of the F3 longwall working. Major factors that influenced the stability of the F3 longwall were taken into account. Based on the obtained results from numerical analysis and the in-situ observations, the stability of the F3 longwall was discussed and evaluated. Consequently, recommended practical actions regarding roof control were put forward for continued operation in the F3 longwall panel.

Keywords: numerical analysis; longwall working stability; powered roof support; failure; in-situ observations

[1] CENTRAL MINING INSTITUTE (GIG), 1 GWARKÓW SQ., 40-166 KATOWICE, POLAND
[2] JASTRZĘBSKA SPÓŁKA WĘGLOWA SA, POLAND

* Corresponding author: pnguyen@gig.eu

1. Introduction

Longwall stability is considered the most difficult and complex engineering problem in underground mining. It determines the conditions of the mining operation and the safety level for miners and has a significant impact on productivity and production costs. Several pieces of research were carried out to analyse the factors affecting the longwall working stability. The weak immediate roof, massive overburden strata, and coal seam thickness are major factors that significantly impact the longwall stability[1-6]. In many cases, the presence of water and dynamic load (seismicity), discontinuities (joints and faults), seam depth and seam inclination were linked to longwall failures [1,2,7-10]. Except for these natural factors, studies also pointed out the importance of human (operating) factors in roof control: canopy tip to face distance, powered roof support capacity and control settings, panel width, extraction height and time [1,2,4,7,11-13]. In fact, longwall mining stability is affected by many factors combined. Each longwall mining case in a given region should be analysed individually due to the complex geological and mining conditions.

In Poland, an empirical method developed by Biliński [14] is commonly applied to assess the stability of the roof in longwall panels whilst selecting the powered roof support for longwalls [1,15-17]. The experience-based method relies on calculations of the roof bearing capacity index 'Ibc', illustrating the ability to maintain their geometric continuity during the longwall mining operation. The value of the roof bearing capacity index is calculated by the following formula:

$$I_{bc} = \frac{1}{\dfrac{\dfrac{0.05}{R_c} + 0.006}{0.012\dfrac{M_P}{M_Q} + 0.002} + 0.3} \tag{1}$$

where: R_c – in-situ compressive strength in a given longwall panel, MPa; M_P – capacity moment of a powered roof support, MNm, M_Q – load moment of the rock mass, MNm.

Values of the 'Ibc' below 0.7 indicate very poor roof maintenance, i.e. high risk of roof fall. Values of 'Ibc' equal to or greater than 0.7 and less than 0.8 indicate the difficult roof maintenance conditions. Values of 'Ibc' equal to or greater than 0.8 indicate proper roof maintenance. According to Eq. (1), the higher the capacity moment of powered roof support is set the higher the value of 'Ibc' is obtained as an outcome. In practice, an increase of pressure in hydraulic legs is a common solution to improve roof conditions.

The methods based on underground measurements and observations can be supplemented with numerical analyses that illustrate the interaction of rock layers in the rock mass and the interaction of the powered roof support with the rock mass surrounding the longwall mining. In recent years, numerical modelling has been increasingly used as an auxiliary tool in solving geotechnical problems, such as assessment of longwall stability and determining the interaction of the powered roof support with the rock mass [7,11,18-26]. By means of numerical modelling, a number of geological and mining factors can be simultaneously taken into consideration, which is not possible in analytical and/or empirical analyses. The numerical calculation results are useful for comparison with the results of laboratory tests and in-situ tests.

During the longwall mining operation at the Borynia-Zofiówka-Jastrzębie (BZJ) coal mine, some roof failures occurred that caused the stoppage. To assess the stability of the F3 longwall working, a numerical analysis was carried out using the finite difference method – code FLAC2D [27]. A numerical model was performed representing the detailed geological and mining conditions around the F3 longwall. Major influencing factors such as pressure in the hydraulic legs, the thickness of weak and stratified roof rock layer, and tip to face distance were taken into account and examined on the F3 longwall. Based on in-situ observations and the obtained results from numerical modelling combined, the stability of the F3 longwall was evaluated, and then, practical activities were proposed for improving the longwall roof conditions during its further mining operation. As the most essential practical action, it is suggested to set the optimal low pressure in the hydraulic legs instead increase the supply pressure acc. to Eq. (1) to improve the roof conditions in the weak geological conditions around the longwall mining such as the F3 longwall.

2. Case study

2.1. Brief characteristics of geological and mining conditions at the studied site

The F3 longwall panel is located in the 406/1 coal seam at the BZJ coal mine, and its outline is defined by: F3 upcut, F3 headgate, F3 tailgate and longwall stop line (Fig. 1). The F3 longwall panel lies at a depth of about 810÷850 m, its longitudinal slope is 0÷6° on N-E, and the thickness is 1.08÷1.40 m [28].

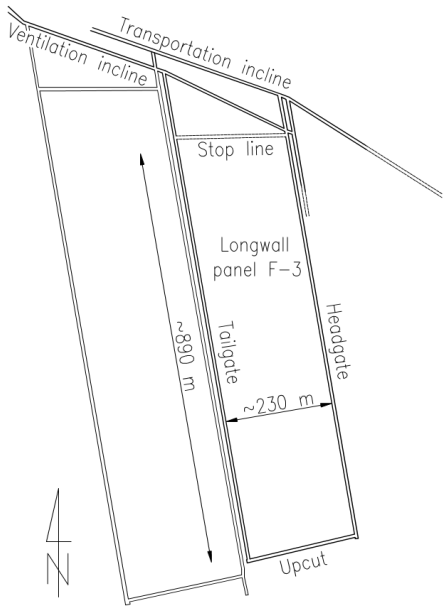

Fig. 1. Outline of the F3 longwall panel in the 406/1 coal seam [28]

According to the given description of geological and mining conditions, roof rocks consist of shale with coal lamina (0.15÷1.4 m), shale or sandy shale with a total thickness (2.0÷12.0 m), shale (0.1÷0.4 m) with coal lamina and a gob of the mined 405/2 coal seam (1.2÷1.5 m). Above the gob, there are layers of shale and sandstone. The vertical distance between the 406/1 and 405/2 seam ranges from 2.0 m (upcut) to 10.0 m (stop line) [28]. In the floor rock, there is shale with coal laminas (0.0÷0.35 m) and sandy shale (2.8÷12.0 m).

The geological profile in the 406/1 coal seam is summarised in Table 1.

TABLE 1

Lithological structure of rock mass around the 406/1 coal seam

	Type of rock	Layer thickness, m	Compressive strength, MPa
Roof rocks	Shale	—	88÷97
	Sandstone	14.0÷19.0	80
	Shale	0.15÷1.65	88÷97
	Consolidated gobs (after the 405/2 coal seam extraction)	1.2÷1.5	12÷20
	Shale with coal lamina	0.1÷0.4	30÷50
	Sandy shale	2.0÷12.0	88÷97
	Shale with coal lamina	0.15÷1.4	30÷50
Coal seam 406/1	Coal	1.08÷1.4	12.8
Floor rocks	Shale with coal lamina	0.0÷0.35	30÷50
	Sandy shale	2.8÷12.0	45÷84
	Sandstone	—	80
	Shale	—	45÷84

2.2. In-situ observations

The observations have been carried out regarding the roof maintenance conditions in the F3 longwall for various values of the powered roof support capacity and the tip to face distance (0.7÷1.5 m). The observation results show that the improvement of roof maintenance conditions was achieved by setting the optimal lower pressure values in the hydraulic legs (up to 25 MPa). This reduced the rock falls from the immediate roof rock. According to the observation report, during the powered roof support sections spragging, the canopy front tip "moved away" from the roof due to excessive penetration of the canopy back tip into the immediate roof rock layer with coal lamina. This situation caused an increase of tip to face distance and, in consequence, rock falls occurred. Steel bars were applied to stop further rock falls (Fig. 2).

The process of such a failure can be illustrated in Fig. 3. In the case of weak and stratified immediate roof rock, the canopy tends to break the roof rock, with rock falls occurring at the beginning in the unsupported part on a small scale (Fig. 3a). If no prevention actions are taken to stop rock falls, then roof rock will fall layer by layer (Fig. 3b), forming a void above the canopy of different sizes (Fig. 3c and Fig. 3d). This leads to a change in the geometry of the powered support where roof maintenance is considered poor.

Fig. 2. A rock fall event in the F3 longwall face

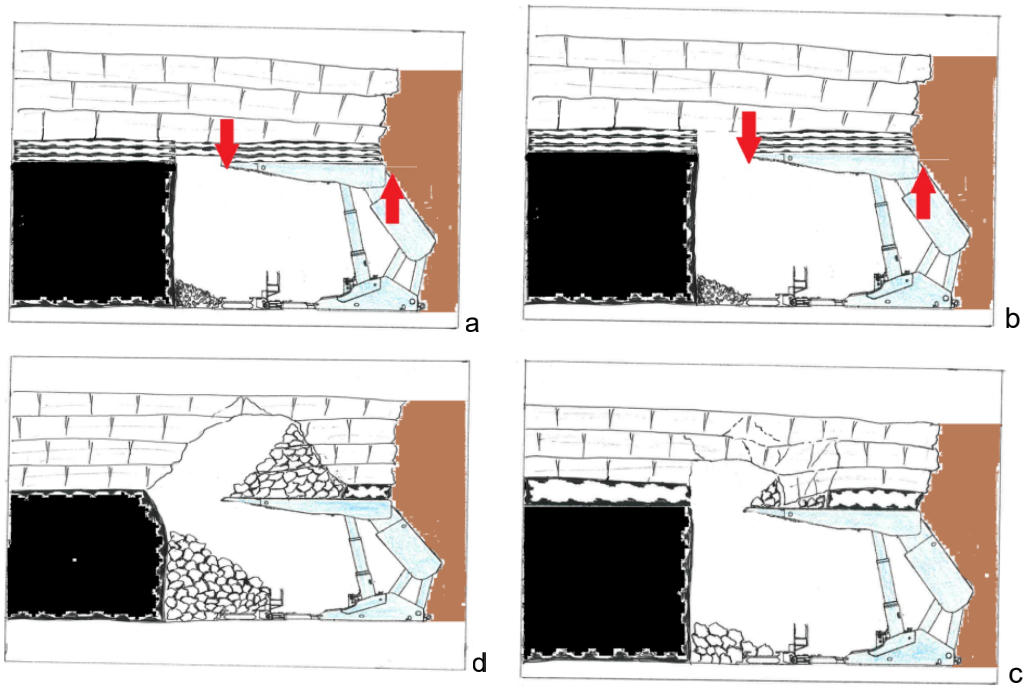

Fig. 3. Graphical interpretation of roof fall in case of setting higher pressure in the hydraulic legs (in sequence: a÷d)

3. Numerical modelling

3.1. Model description

In the model, in accordance with the geological and mining conditions, the F3 longwall with a mining height of 2.0 m lies at an average depth of 830 m. The distance between the 406/1 seam and the 405/2 seam (or its gob) was 2 m. Fig. 5 shows the outline of the two-dimensional numerical model and the location of the rock layers surrounding the F3 longwall. In all of the considered models, the exact block was cut out from the rock mass, which is a two-dimensional deformation state. The model was divided into over 10,000 elements and had dimensions of 80 m by 40 m (Fig. 4).

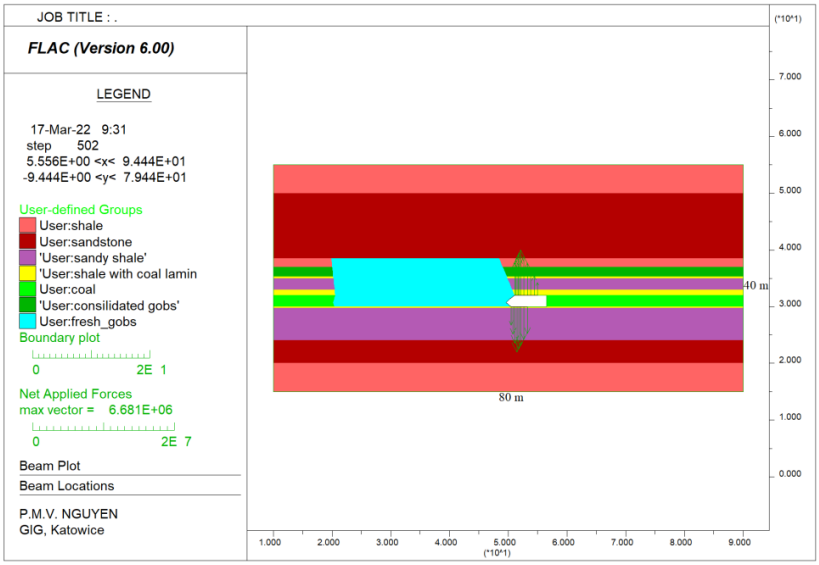

Fig. 4. Model geometry and location of individual rock layers in FLAC2D

The initial horizontal stress is assumed to be equal to the vertical stress. The initial stress value was calculated by the formula presented by Biliński [29] that described the geological and mining conditions in Poland:

$$q = 0.02 \cdot H \cdot m_c \cdot \cos\alpha \tag{2}$$

where q the primary pressure, MPa; H the mining depth, m; m_c is a factor with a calculated value of 1.0 for region of the BZJ coal mine (Upper Silesian Coal Basin, Poland) and α the coal seam inclination, °

According to the reconsolidation tests carried out for gob formed after the exploitation of longwall panels located in the 405/2 coal seam, the degree of gob reconsolidation can be determined as the optimal and equivalent compressive strength of consolidated gob was determined at

12.25 MPa. Thus, it is reviewed that the gob was consolidated and became a load-bearing layer. The structure of consolidated gob behaves like such a structure of solid rocks (PROSAFECOAL) [30].

The rock mass is modelled as a Mohr-Coulomb material using the built-in constitutive model available in FLAC2D. A summary of the material properties used in this model is presented in Table 2.

TABLE 2

Mechanical parameters of intact rocks at the BZJ coal mine

Type of rocks	Bulk modulus K (GPa)	Shear modulus G (GPa)	Angle of internal friction θ (deg.)	Cohesion c (MPa)	Tensile strength R_t (MPa)	Density ρ (kg/m^3)
Sandstone	8.0	5.6	30	7.8	4.0	2600
Shale	4.8	3.0	28	4.0	2.0	2700
Sandy shale	6.0	3.5	28	6.4	2.4	2700
Shale with coal lamina	3.6	2.0	26	3.6	1.2	2500
Coal	2.5	1.15	25	3.2	1.0	1300
Consolidated gobs	2.0	1.1	20	2.0	0.7	2200

3.2. Modelling of caved zone induced by longwall mining

Determining the geometry of the caved zone was the subject of a number of studies that were later used to develop various empirical formulas (Table 3).

TABLE 3

Hypotheses for calculating thickness of caved zone

Author, year	Peng and Chaing, 1984 [31]	Bai et al., 1995 [32]	Mazurkiewicz et al., 1997 [33]	Heasley, 2004 [34]	Biliński, 2005 (simplified) [29]	Wang et al., 2017 [35]
Thickness of caved zone	$(2 \div 10)t$	$\frac{100t}{c_1 g + c_2}$	$\frac{t}{k_r - 1}$	$(10 \div 18)t$	$\frac{nk_s t}{0.05R_c^{0.5} + 0.02}$	$(3 \div 4)t$

t – thickness of coal seam,
c_1, c_2 – constants dependent on the compressive strength of roof rocks [32],
k_r – 1.15÷1.5 for geological and mining conditions in Polish mines,
n – coefficient of intensity of movements in the area of destressed rock mass, $n = 2$ in the case of full caved longwall mining,
k_s – compressibility factor of gob, $k_s = 0.8$ for caved zone,
R_c – weighted average compressive strength of roof rocks

The height of the caved zone tends to be proportional to the thickness of the exploited seam. The variety of hypotheses is considerable due to the different mining conditions in which the research was conducted. However, only Biliński [29] and Bai et al., [32] considered the compressive strength of roof rocks to estimate the height of the caved zone. Therefore, these hypotheses are considered the most reliable for determining the geometry of a caved zone induced by longwall mining.

Access to the caved zone is limited. Therefore, it is very difficult to find the equivalent mechanical properties that are reliable to express the heterogeneity of these materials. Various

studies were carried out to determine the equivalent mechanical properties of the caved zone. The elastic modulus of this zone can be calculated as a function of the compressive strength of undisturbed roof rocks and the bulking factor [34]. Tajduś [37] used the back analysis method to determine the value of parameters of a disturbed rock mass caused by mining. He found that the elastic modulus in the horizontal and vertical directions is very low and ranges from 50 MPa to 150 MPa. Cheng et al., [38] and Jiang et al., [39] assumed that the elastic modulus and Poisson's ratio in the caved zone are 190 MPa and 0.25. Ahmed et al., [40] suggested that the elastic modulus of the caved zone is about 2.1% of the elastic modulus of roof rocks. In this manuscript, the caved zone was modelled as an elastic material with the adopted elastic modulus (Young's modulus) and Poisson's ratio is 200 MPa and 0.4, relatively.

3.3. Modelling of powered roof support

The force values occurring in nodes of the powered roof support affect the stress values and determine the entire structure with the change of the support's resistance. Calculation of the distribution of load along the powered roof support canopy and base was carried out for forces caused by the rock mass pressure. These forces are dependent on the pressure set in the hydraulic legs and the geometry of powered roof support [41]. The methodology for the powered roof support modelling in longwall mining relies on applying the computed distribution of forces [6,42-46]. The powered roof support was simulated in FLAC2D using a beam profile modelled, including the load with values and distribution on the powered roof support canopy and base.

3.4. Model validation

The abutment pressure distribution around the F3 longwall face is shown in Fig. 5. In the caved zone, the vertical stress gradually increases to a value close to the initial vertical stress (16.6 MPa). The maximum value of the vertical stress (approx. 26 MPa) is approx. 1.5 times

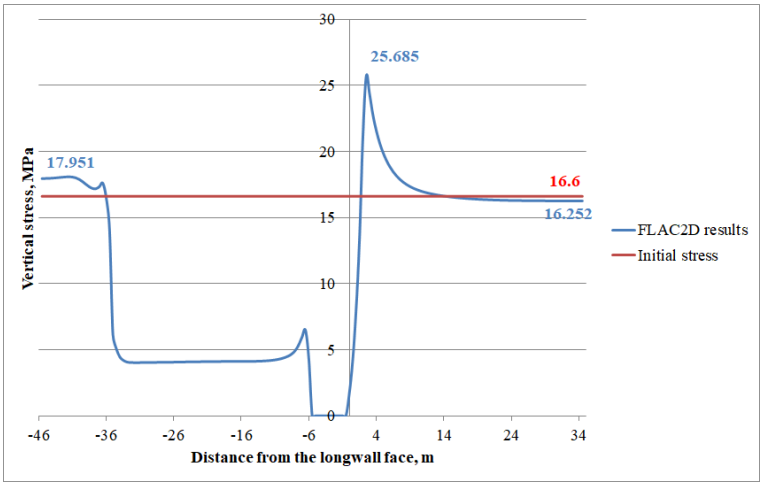

Fig. 5. Vertical stress distribution around the F3 longwall face

the value of the initial vertical stress. It is located approx. 4 m in front of the longwall face. Then, the vertical stress gradually reduces to the value of the initial vertical stress in front of the longwall face. The simulation results are in good agreement with the results presented by other authors [47-51]. Thus, the modelling methodology, the adopted mechanical rock parameters and material models can be considered appropriate for further numerical calculations in this manuscript.

3.5. Variants of numerical calculation

To assess the stability of the F3 longwall working, the following major influencing factors include powered roof support capacity and control settings (pressure in the hydraulic legs), the thickness of weak and stratified roof rock layer, and the tip to face distance were taken into account. Based on the actual geological and mining conditions in the F3 longwall panel, the thickness of weak and stratified roof rock layer with a value of 0.3, 0.6 and 1.0 m, tip to face distance with a value of 0.5, 1.0 and 1.5 m were taken into numerical calculations. The selected powered roof support for the F3 longwall is equipped with two legs with an internal diameter of 350 mm; canopy length is 3.820 m; coefficient of friction between the rock mass and powered support: $\mu = 0.3$; operating height range is 1.1÷2.2 m; width is 1.75 m. Pressure in the hydraulic legs with values of 11.5 MPa, 25 MPa and 38 MPa were taken into numerical consideration. For such pressure in the hydraulic legs, appropriate models were created to determine the values and distribution of load-bearing capacity along with the support canopy and base. The distribution of load-bearing capacity and its values are shown in Fig. 6.

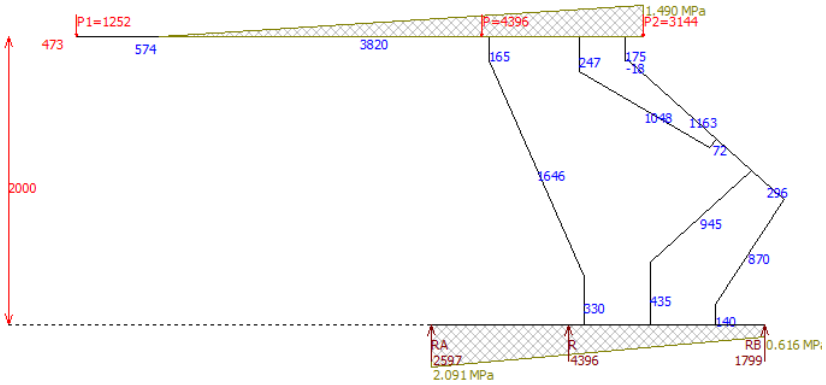

Fig. 6. The value and distribution of load-bearing capacity of the powered roof support for an example of 25 MPa pressure set in the hydraulic legs

The roof rocks of the 406/1 coal seam could be fractured or even caved by the longwall operation in the 405/2 coal seam above. Therefore, calculations were conducted for two main scenarios (considerations):

(I) the immediate roof layers above the 406/1 coal seam are undisturbed.
(II) the immediate roof layers above the 406/1 coal seam are disturbed. This means the strength parameters of the immediate roof rocks above the F3 longwall will be reduced.

Variants of numerical calculation are summarised in Fig. 7.

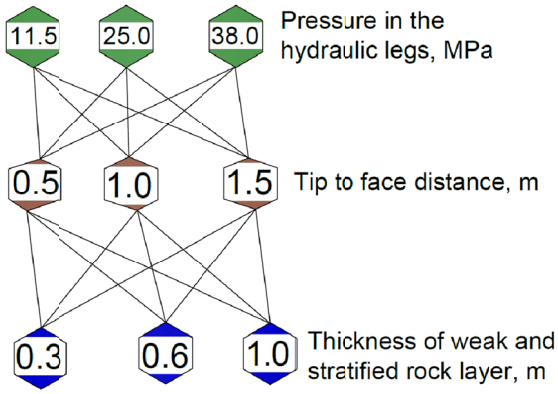

Fig. 7. Calculation variants for assessing the stability of the F3 longwall for 2 scenarios

4. Results analysis

The results of the numerical calculations were presented in the form of maps of plasticity indicators and maps of displacements around the longwall face. Due to a large number of obtained results, only selected maps for certain calculation variations are shown in this manuscript.

4.1. The immediate roof layers above the 406/1 coal seam are undisturbed

The thickness of shale with coal lamina of 1 m was modelled. An example of results is shown in Figures 6 and 7. With the distance of tip to the face of 0.5 m, the vertical displacement decreased with the increase of pressure in the hydraulic legs from 11.5 MPa to 38 MPa (Fig. 8-displacement), and the size of the failure zone around the longwall face is reduced (Fig. 8-plasticity). In the case of pressure in the hydraulic legs set at 25 MPa, the vertical displacement increased with the increase of tip to face distance (Fig. 9-displacement), while the size of the failure zone around the longwall face was also larger (Fig. 9-plasticity). Maps of plasticity indicators confirm the same tendency of rock mass behaviour that vertical displacements do.

A comparison of vertical displacements around the longwall face in the case of 1.0 m thick shale with coal lamina is presented in Fig. 10.

Vertical displacements (Fig. 10) indicate the influence of tip to face distance and load-bearing capacity of the powered roof support on rock mass behaviour around the longwall face. The more pressure set in the hydraulic legs, the less vertical displacement of roof and floor obtained. The more distance of tip to face set, the more vertical displacement of roof and floor obtained.

Thickness of shale with coal lamina of 0.6 m and 0.3 m were also modelled. Summary of results is shown in Figs. 11 and 12.

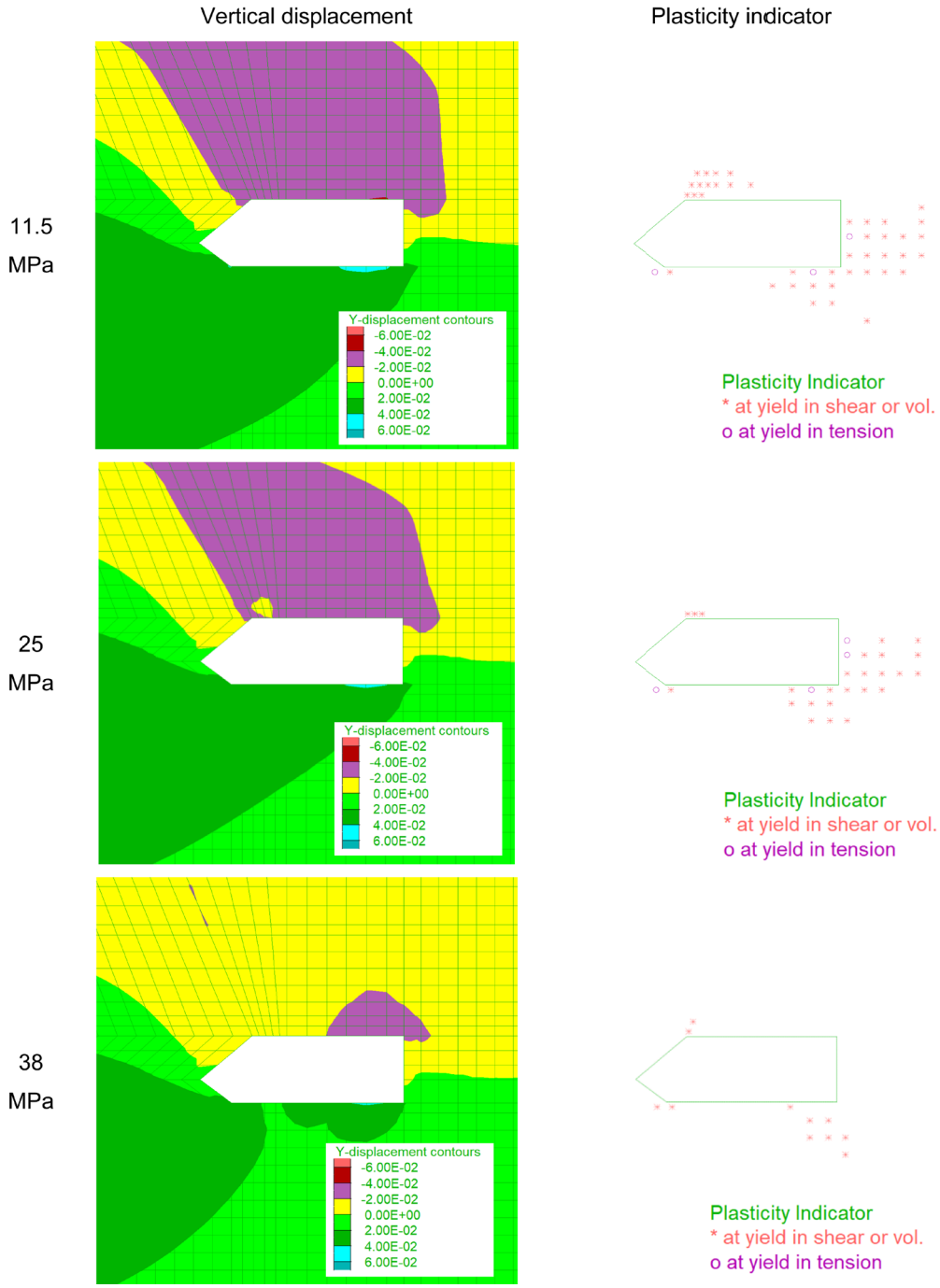

Fig. 8. Map of vertical displacement around the longwall face with different values of pressure in the hydraulic legs (tip to face distance of 0.5 m)

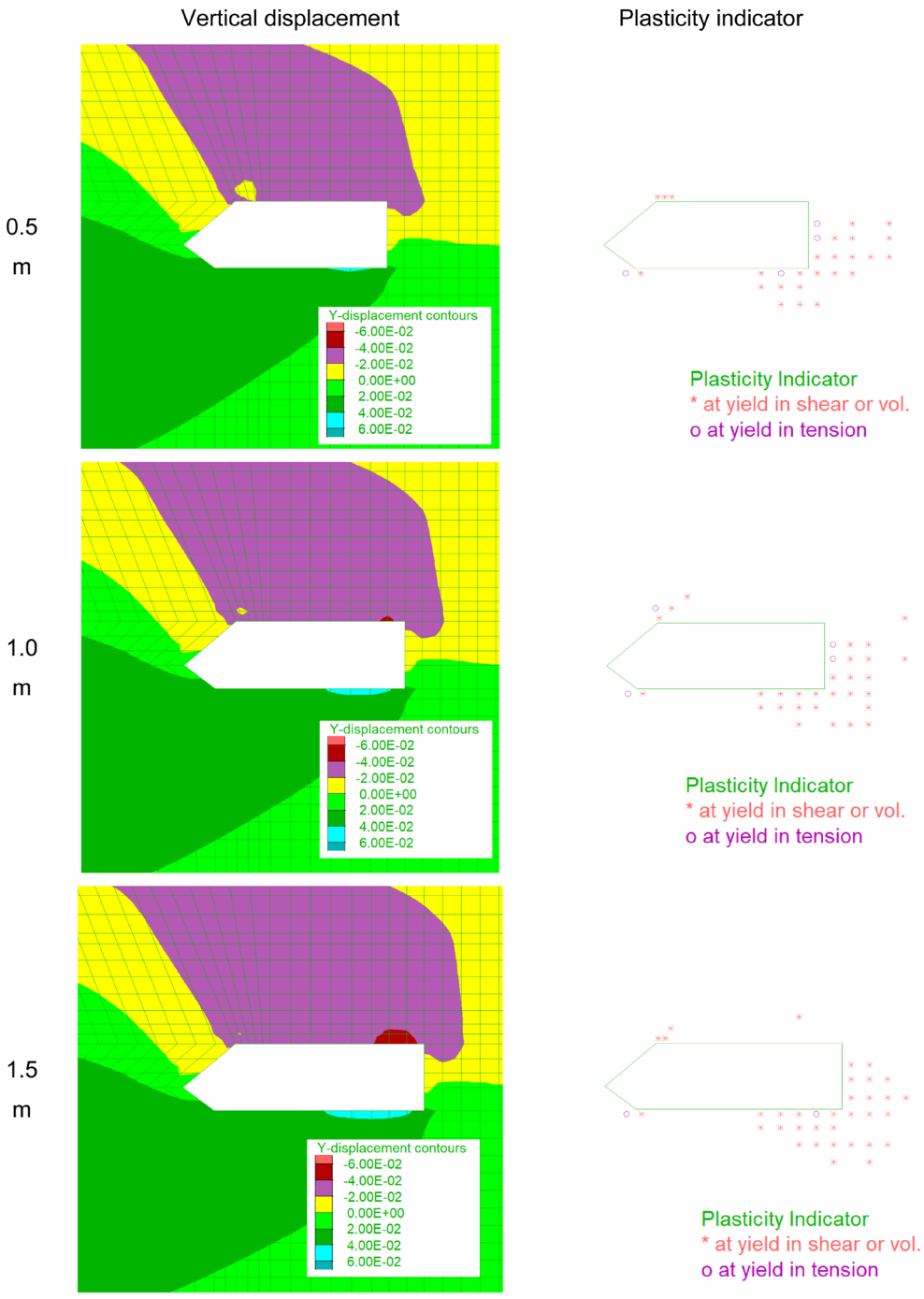

Fig. 9. Map of vertical displacement around the longwall face with different tip to face distance (pressure in the hydraulic legs was set at 25 MPa)

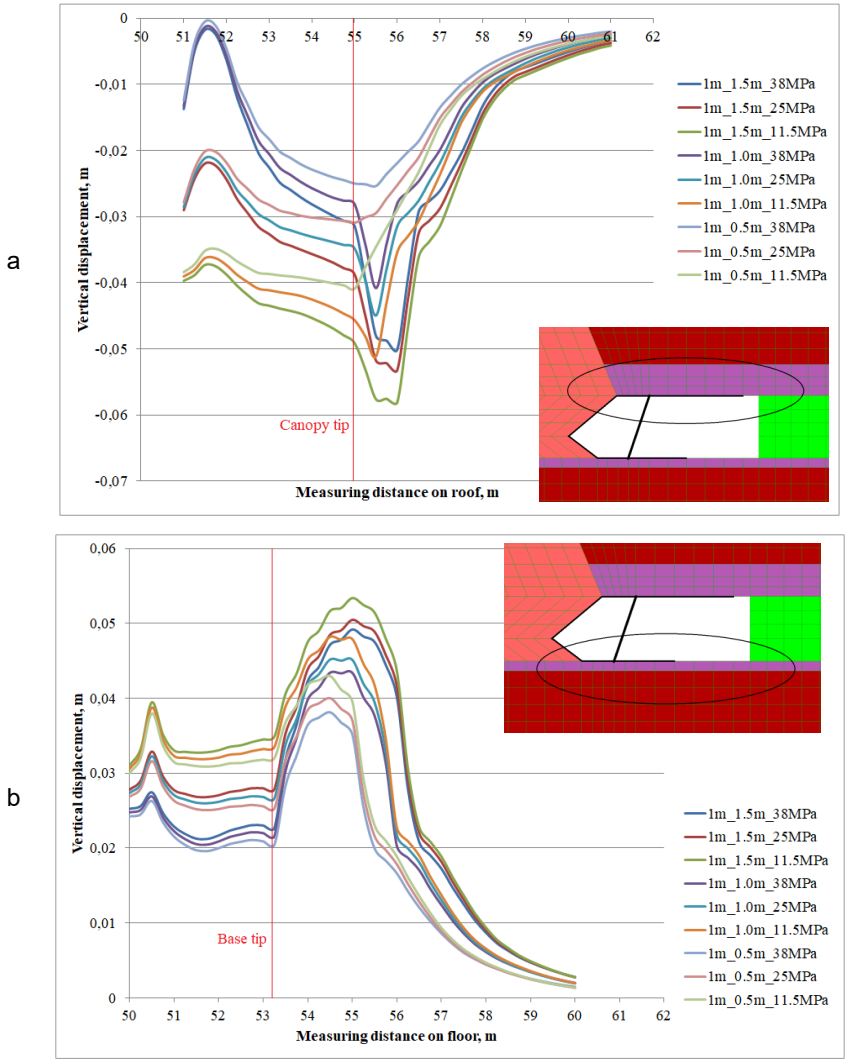

Fig. 10. Vertical displacement around the longwall face in the case of 1.0 m thick shale with coal lamina: a) roof; b) floor

The obtained results indicate that:

– Displacements around the longwall facet tend to reduce with the increase of load-bearing support capacity (pressure in the hydraulic legs) and the decrease of the tip to face distance, which have a positive effect on the longwall stability.
– Displacements on the roof slightly increased with the increase of thickness of the shale layer with coal lamina (Fig. 10a, 11a, 12a). On the other hand, displacements on the floor decreased with the increase of thickness of the shale layer with coal lamina (Fig. 10b, 11b, 12b).

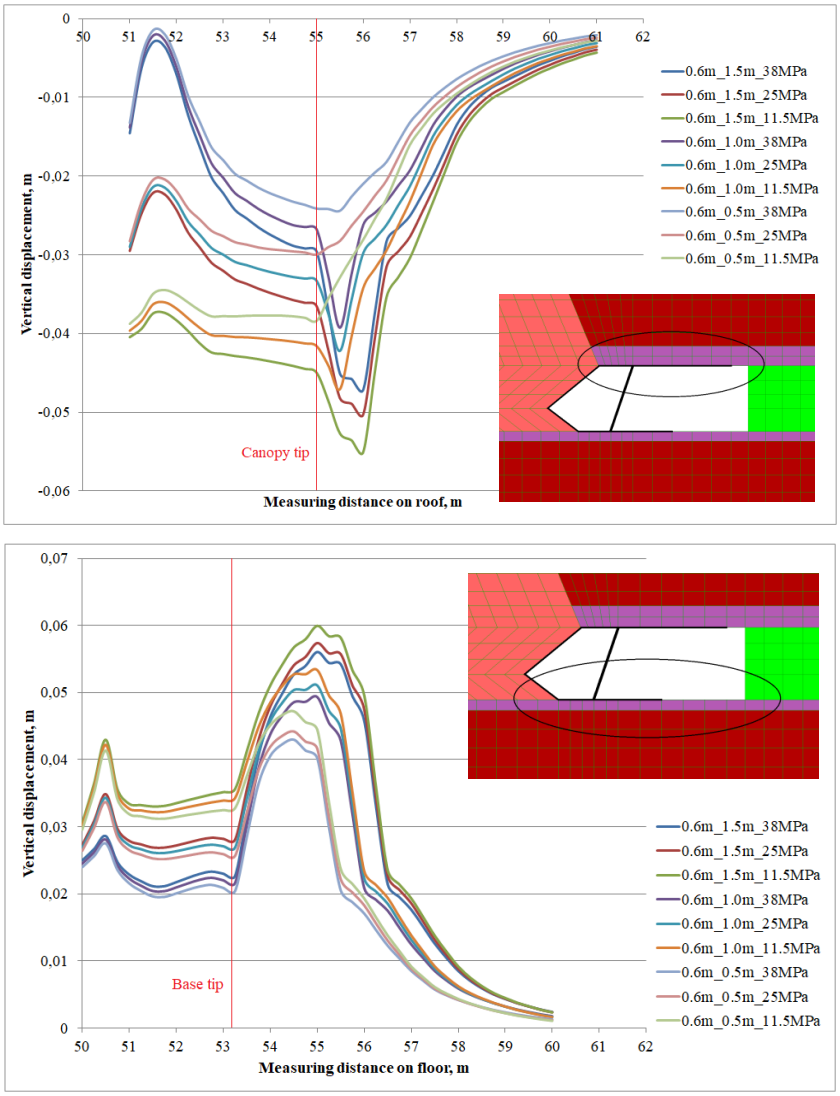

Fig. 11. Vertical displacement around the longwall face in the case of 0.6 m thick of shale with coal lamina: a) roof; b) floor

The obtained results, in this case, have confirmed the tendency of the impact of tip to face distance and load-bearing capacity of support on roof rock behaviour as presented in many other studies and mining practices, i.e. short tip to face distance and high pressure in the hydraulic legs tend to improve the roof maintenance conditions of the longwall mining. However, they did not show the actual events (failures) that were observed in the F3 longwall face during its operation.

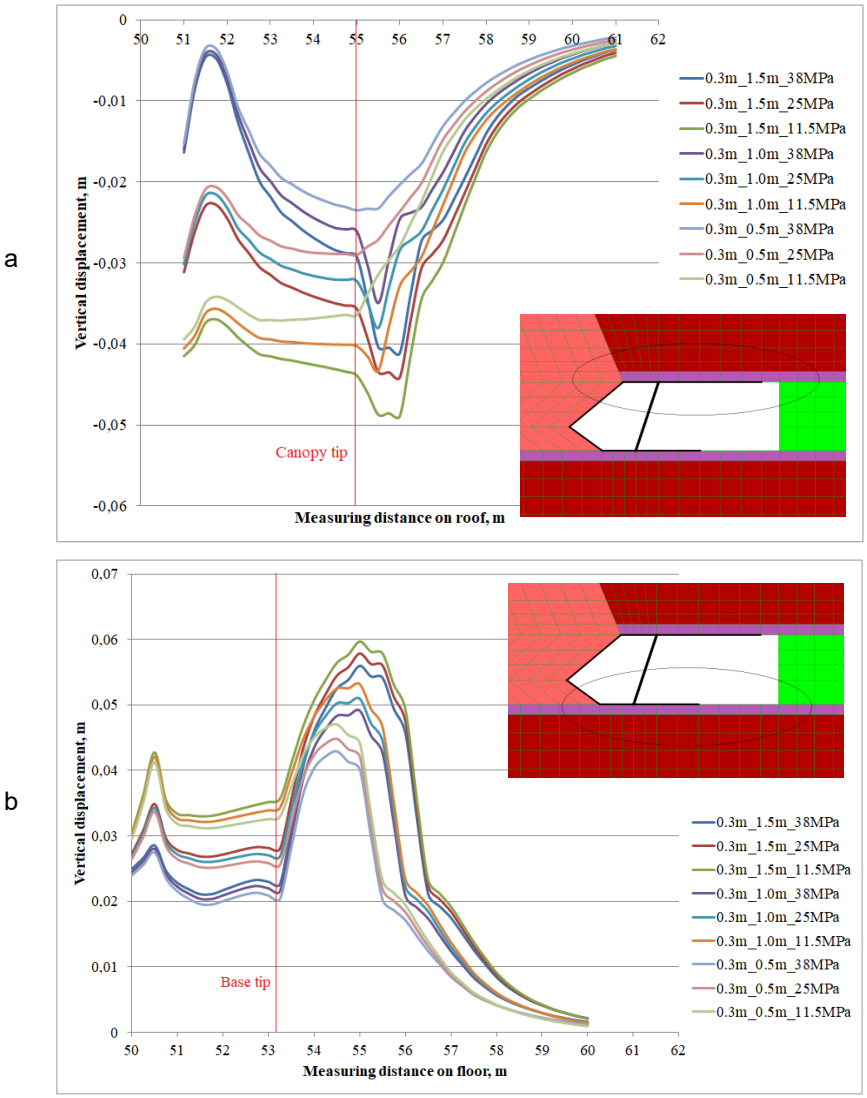

Fig. 12. Vertical displacement around the longwall face in the case of 0.3 m thick of shale with coal lamina: a) roof; b) floor

4.2. The immediate roof layers above the 406/1 coal seam are disturbed

The further calculations were carried out by considering the fractured immediate roof rocks located above the F3 longwall as a result of the longwall mining operation in the 405/2 coal seam. As an example, the mechanical parameters of shale with coal lamina were reduced by 50%. All variations were recalculated. The summary of the results is shown in Figs. 13, 14, and 15.

In general, these results show the same tendency of the impact of tip to face distance on rock

a

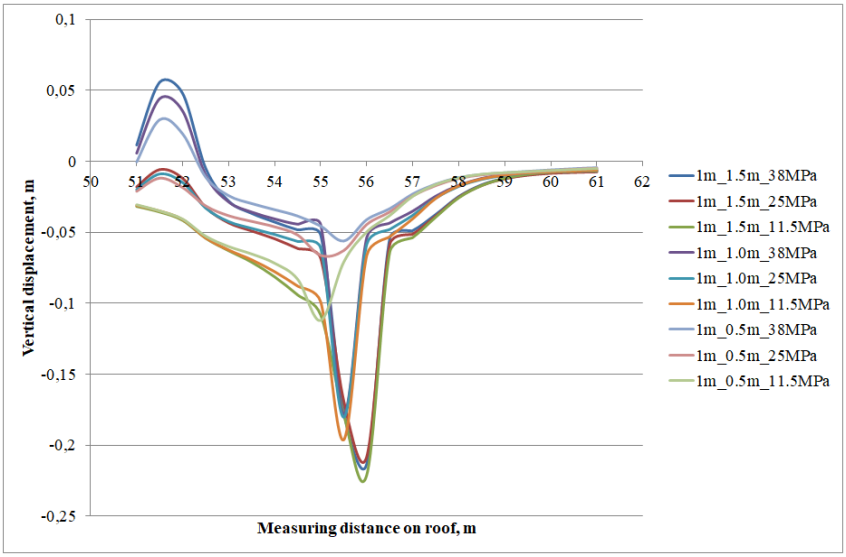

b

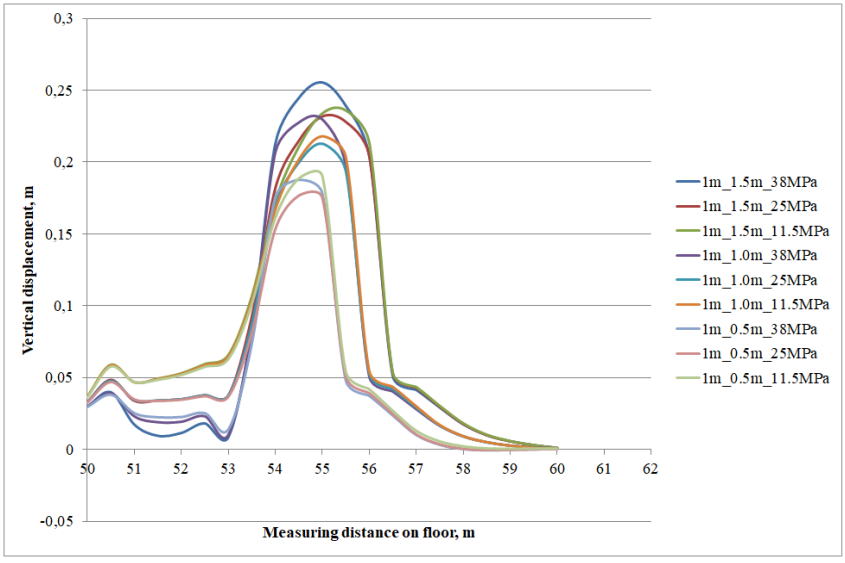

Fig. 13. Vertical displacement around the longwall face in the case of 1.0 m thick of shale with coal lamina: a) roof; b) floor

roof behaviour as shown in Chapter 4.1, i.e. the vertical displacements around the F3 longwall face increased with the increase of the tip to face distance (Figs. 13-15). The thickness of the shale layer with coal lamina has no significant impact on roof rock behaviour, i.e. the vertical displacements on roof rock and floor rock slightly increased with the increase of thickness of the shale layer (Figs. 13-15). However, the tendency of the impact regarding pressure in the hydraulic legs is opposite the case presented in Chapter 4.1, i.e. vertical displacements on the floor

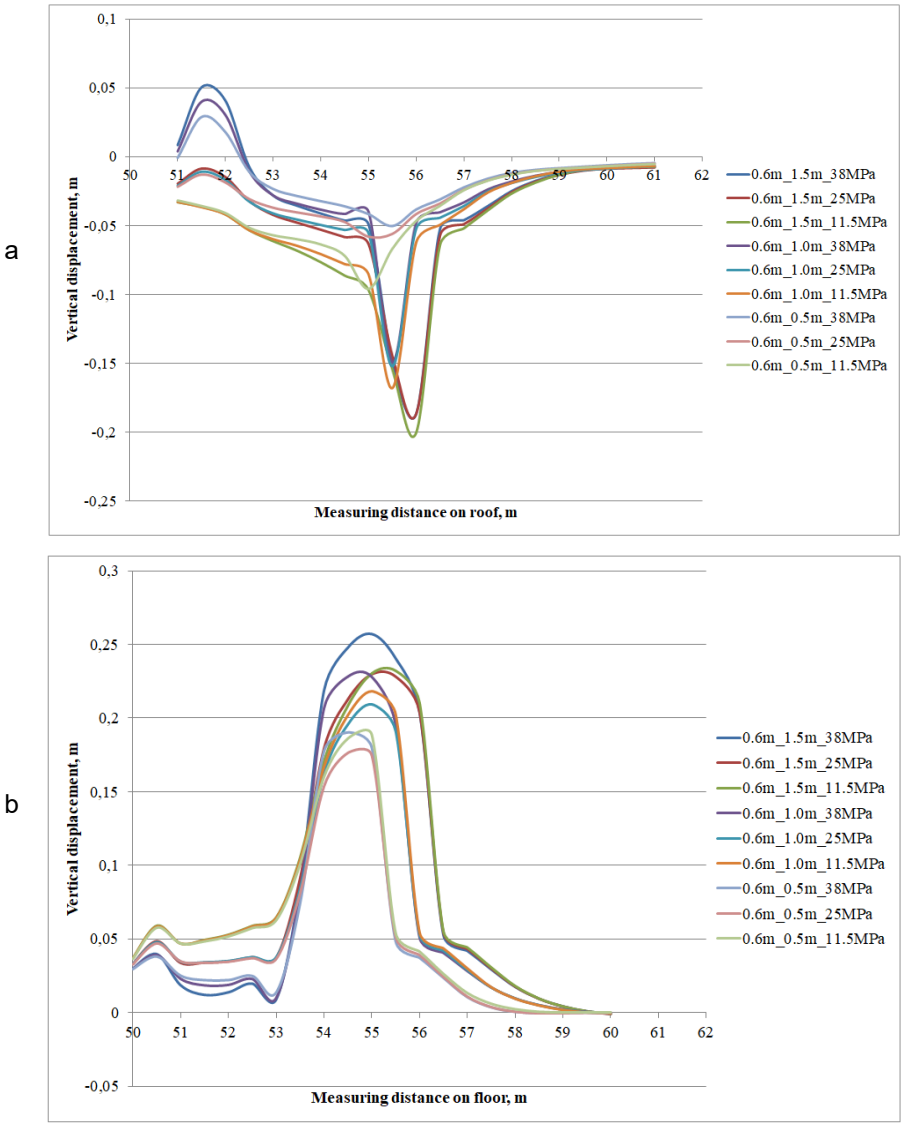

Fig. 14. Vertical displacement around the longwall face in the case of 0.6 m thick of shale with coal lamina: a) roof; b) floor

in case of higher pressure (38 MPa) are greater than the vertical displacements on the floor in the case of 11.5 MPa and 25 MPa, apparently in case of long tip to face (1.0÷1.5 m) (Figs. 13b, 14b, 15b). Moreover, despite the vertical displacements on the roof rock reduced with the increase of pressure on the hydraulic legs, the back part of the roof rock has 'moved up' – with the positive values of vertical displacements on roof rock in case of higher pressure (Figs. 13a, 14a, 15a). It means that the canopy's back tip penetrated into the roof rock and the canopy's front tip

a

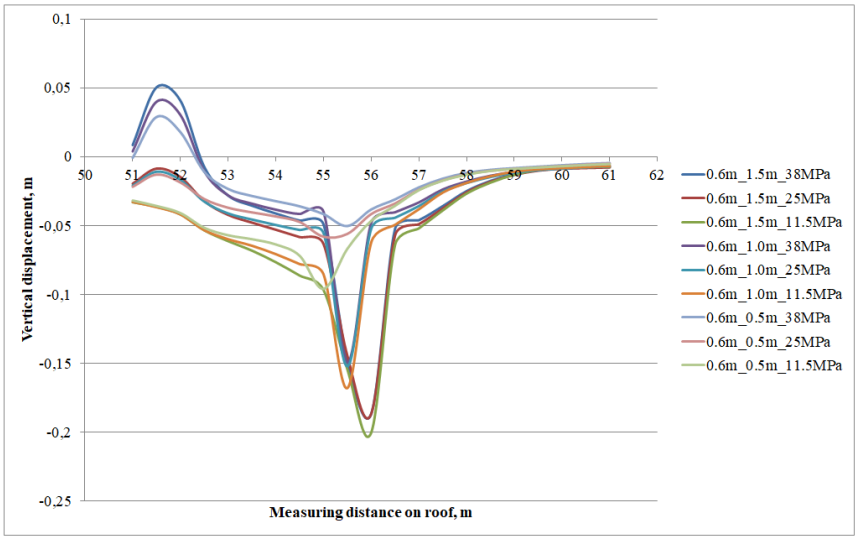

b

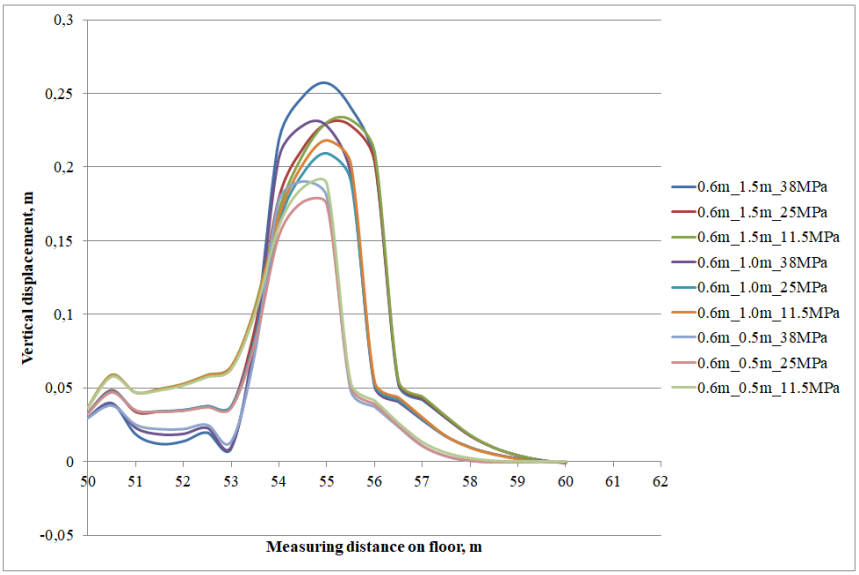

Fig. 15. Vertical displacement around the longwall face in the case of 0.3 m thick of shale with coal lamina: a) roof; b) floor

moved down. In other words, the powered support does not sufficiently interact with roof rock, and it leads to improper dimensions and geometrical parameters of the powered support, which significantly impacts the further longwall mining operation. Such an event was observed and reported as the observation results introduced in Chapter 2.2. Hence, in the case of weak roof rock, it is suggested to maintain the small distance of tip to face as possible (e.g. 0.5 m) and the optimal low pressure in hydraulic legs such as 25 MPa.

5. Conclusions and practical recommendations

From assessing the longwall face stability, a numerical analysis was carried out using the finite difference method code – FLAC2D for the F3 longwall at the BJZ coal mine. The actual geological and mining conditions and various influencing factors were taken into account, i.e. the tip to face distance, the thickness of the weak roof rock layer, as well as the shield resistance force. Based on the numerical calculations and the in-situ observations, the following conclusions and recommendations can be drawn:

- the obtained results confirm the impact of the major influencing factors such as weak immediate roof, canopy tip to face distance, powered roof support capacity and control settings on roof rock behaviour in longwall face,
- in the case of undisturbed immediate roof rock, numerical modelling results indicate that increasing pressure in the hydraulic legs tends to improve roof condition. It is matched with the tendency of Biliński's method (Eq. 1). However, in the case of weak immediate roof rock (disturbed), increasing pressure in the hydraulic legs does not improve roof condition because the canopy tends to cut off and penetrate into the weak immediate roof rocks and lead to a change in the required geometry of the powered roof support sections, resulting in rock falls above the canopy. Therefore, the given method is not a proper method for such a case of longwall design and powered roof support selection.
- since the immediate roof of the F3 longwall in the 406/1 seam consists of thin layers of shale with coal lamina, which has fractured and stratified as a result of the exploitation of the 405/2 coal seam (about 2.0 m above), it is crucial to focus particular attention on the method of the powered roof support spragging and shifting during longwall operation. It is suggested to maintain the proper geometry of the powered roof support section by limiting the tip to face distance (to 0.5 m) and setting the optimal low pressure in hydraulic legs (up to 25 MPa).
- numerical calculations, together with in-situ observations and measurements, allowed determining and a better understanding of the mechanisms regarding the interaction of powered support with the rock mass surrounding longwall mining,
- in general, a 2D model managed to assess the longwall working stability in this case study. However, as the rock mass is a spatial and complex structure, three-dimensional numerical modelling should be applied in future work.

References

[1] S. Prusek, S. Rajwa, A. Wrana, A. Krzemień, Assessment of roof fall risk in longwall coal mines. International Journal of Mining, Reclamation and Environment **31** (8), 558-574 (2017). DOI: https://doi.org/10.1080/17480930.2016.1200897

[2] T.P. Medhurst, Practical considerations in longwall support behaviour and ground response. Proceedings of the 5th Coal Operators' Conference, Wollongong, New South Wales, pp. 49-58 (2005).

[3] T.M. Barczak, Examination of design and operation practices for longwall shields. Bureau of Mines Information Circular, USA.IC.9320 (United State Department of the Interior) (1992).

[4] R. Frith, A holistic examination of the load rating design of longwall shields after more than half a century of mechanized longwall mining. Int. J. Min. Sci. Technol. **25** (5), 687-706 (2015). DOI: https://doi.org/10.1016/j.ijmst.2015.07.001

[5] Y.M. Jiang, B. Wells, Analysis of geologic and geotechnical conditions and their effects on longwall mining to optimize mine planning at Shoal Creek mine. Proceedings of the 17th International Conference on Ground Control in Mining, Wollongong, New South Wales, pp. 54-62 (1998).

[6] J. Wang, Z. Wang, Systematic principles of surrounding rock control in longwall mining within thick coal seams. International Journal of Mining Science and Technology **29** (1), 65-71 (2019). DOI: https://doi.org/10.1016/j.ijmst.2018.11.014

[7] R. Trueman, G. Lyman, A. Cocker, Longwall roof control through a fundamental understanding of shield-strata interaction. International Journal of Rock Mechanics and Mining Sciences **46** (2), 371-380 (2009). DOI: https://doi.org/10.1016/j.ijrmms.2008.07.003

[8] T. Cichy, S. Prusek, J. Świątek, D. Apel, Y. Pu, Use of Neural Networks to Forecast Seismic Hazard Expressed by Number of Tremors Per Unit of Surface. Pure Appl. Geophys. **177**, 5713-5722 (2020). DOI: https://doi.org/10.1007/s00024-020-02602-0

[9] S.X. Hu, L.Q. Ma, J.S. Guo, P.J. Yang, Support-surrounding rock relationship and top-coal movement laws in large dip angle fully-mechanized caving face. Int. J. Min. Sci. Technol. **28** (3), 533-539 (2018). DOI: https://doi.org/10.1016/j.ijmst.2017.10.001

[10] S. Prusek, W. Masny, Analysis of damage to underground workings and their support caused by dynamic phenomena. J. Min. Sci. **51** (1), 63-72 (2015). DOI: https://doi.org/10.1134/S1062739115010093

[11] S. Rajwa, T. Janoszek, S. Prusek, Influence of canopy ratio of powered roof support on longwall working stability – A case study. Int. J. of Min. Sci. and Technol. **29** (4) (2019). DOI: https://doi.org/10.1016/j.ijmst.2019.06.002

[12] S. Rajwa, T. Janoszek, S. Prusek, Model tests of the effect of active roof support on the working stability of a longwall. Computers and Geotechnics **118** (5), 103302 (2020). DOI: https://doi.org/10.1016/j.compgeo.2019.103302

[13] C. Liu, H.M. Li, D.J. Jiang, Numerical simulation study on the relationship between mining heights and shield resistance in longwall panel. Int. J. Min. Sci. Technol. **27** (2), 293-297 (2017). DOI: https://doi.org/10.1016/j.ijmst.2017.01.017.

[14] A. Biliński, Manifestations of rock mass pressure in longwall mining panel in coal seams (in Polish). Politechnika Śląska, Zeszyt Naukowy nr 221, Górnictwo z. 31, Gliwice (1968).

[15] S. Prusek, S. Rajwa, W. Kasperkiewicz, T. Budniok, Assessment of performance of powered shield support used on weak floor, World Mining Congress, Montréal (2013).

[16] S. Rajwa, M. Płonka, Z. Lubosik, A. Walentek, W.Masny, Principles of safe use of powered supports, Proceedings of the School of Underground Mining, Ukraina (2008).

[17] M. Płonka, S. Prusek, K. Rułka, 3D strata model application for the selection method of the support for longwall excavation, III International Conference Mining Techniques, Kraków – Krynica, 233-245 (2003).

[18] S.R. Islavath, D. Deb, H. Kumar, Life cycle analysis and damage prediction of a longwall powered support using 3D numerical modelling techniques. Arabian Journal of Geosciences **12** (14), (2019). DOI: https://doi.org/10.1007/s12517-019-4574-y

[19] S. Prusek, M. Płonka, A. Walentek, Applying the ground reaction curve concept to the assessment of shield support performance in longwall faces. Arab. J. Geosci. **9** (3), (2016). DOI: https://doi.org/10.1007/s12517-015-2171-2

[20] M. Witek, S. Prusek, Numerical calculations of shield support stress based on laboratory test results. Computers and Geotechnics **72**, 74-88 (2016). DOI: https://doi.org/10.1016/j.compgeo.2015.11.007

[21] Q.S. Bai, S.H. Tu, X.G. Zhang, Numerical modelling on brittle failure of coal wall in longwall face – a case study. Arab. J. Geosci. **7** (12), 5067-5080 (2014). DOI: https://doi.org/10.1007/s12517-013-1181-1

[22] A.K. Verma, D. Deb, Numerical Analysis of an Interaction between Hydraulic-Powered Support and Surrounding Rock Strata. International Journal of Geomechanics **13** (2), (2013). DOI: https://doi.org/10.1061/(ASCE)GM.1943-5622.0000190

[23] G.S.P. Singh, U.K. Singh, Influence of strata characteristics on face support requirement for roof control in longwall workings – a case study, Mining Technology, Transactions of the Institutions of Mining and Metallurgy: Section A. **121** (1) (2012). DOI: https://doi.org/10.1179/174328611X13061613463896

[24] G.S.P. Singh, U.K. Singh, Prediction of caving behaviour of strata and optimum rating of hydraulic powered support for longwall workings. International Journal of Rock Mechanics and Mining Sciences **47** (1), 1-16 (2010). DOI: https://doi.org/10.1016/j.ijrmms.2009.09.001

[25] T.G. Sitharam, V.B. Maji, A.K. Verma, Equivalent continuum analyses of jointed rockmass, 40th US Symposium on Rock Mechanics (USRMS): Rock mechanics for energy, mineral and infrastructure development in the Northern Regions, Alaska, pages 25-29 (2005).

[26] P. Sharma, A.K. Verma, P. Gautam, Stability analysis of underground pillar in the presence of overlying dump: a case study. Arabian Journal of Geosciences **13** (5), 1-13 (2020). DOI: https://doi.org/10.1007/s12517-020-5133-2

[27] FLAC2D, Version 6.0, Itasca Consulting Group Inc., Minneapolis; software available at www.itascacg.com (2008)

[28] Central Mining Institute (GIG), Research and development documentation (in Polish), Katowice (2017) (unpublished).

[29] A. Biliński, Method of selection of longwall face and roadway supports for the panelling conditions (in Polish). Prace naukowe – Monografie CMG KOMAG. Gliwice (2005).

[30] PROSAFECOAL, Increased productivity and safety of European coalmines by advanced techniques, knowledge and planning tools enabling strata control of the face-roadway junction. Projektu PROSAFECOAL realizowany w ramach Funduszu Badawczego dla Węgla i Stali (Research Fund for Coal and Steel) nr kontraktu RFCR-CT-2007-00001 (2007-2010).

[31] S.S. Peng, H.S. Chaing, Longwall Mining, John Wiley and Sons, Inc., New York (1984).

[32] M. Bai, F. Kendorski, D. Van Roosendaal, Chinese and North American high-extraction underground coal mining strata behavior and water protection experience and guidelines. The 14th International Conference on Ground Control in Mining, Morgantown (1995).

[33] M. Mazurkiewicz, Z. Piotrowski, A. Tajduś, Lokowanie odpadów w kopalniach podziemnych. cz. II Geoinżynieria. Biblioteka Szkoły Eksploatacji Podziemnej, s. 129 (1997).

[34] K. Heasley, A review of Subsidence and Fire Potential at the Major Battery Site, Report no. 2004-P-0017 (2004).

[35] H. Wang, D. Zhang, X. Wang, W. Zhang, Visual exploration of the spatiotemporal evolution law of overburden failure and mining-induced fractures: A case study of the Wangjialing coal mine in China. Minerals **7**, 35 (2017). DOI: https://doi.org/10.3390/min7030035

[36] H. Yavuz, An estimation method for cover pressure re-establishment distance and pressure distribution in the goaf of longwall coal mines. Journal of Rock Mechanics and Mining Sciences and Geomechanics **41** (2), 193-205 (2004). DOI: https://doi.org/10.1016/S1365-1609(03)00082-0

[37] K. Tajduś, New method for determining the elastic parameters of rock mass layers in the region of underground mining influence. Int. J. Rock Mech. Mining Sci. **46** (8), 1296-1305 (2009). DOI: https://doi.org/10.1016/j.ijrmms.2009.04.006

[38] Y.M. Cheng, J.A. Wang, G.X. Xie, W.B. Wei, Three-dimensional analysis of coal barrier pillars in tailgate area adjacent to the fully mechanized top caving mining face. Int. J. Rock Mech. Mining Sci. **47** (8), 1372-1383 (2010). DOI: https://doi.org/10.1016/j.ijrmms.2010.08.008

[39] Y. Jiang, H. Wang, S. Xue, Y. Zhao, J. Zhu, X. Pang, Assessment of mitigation of coal bump risk during extraction of an island longwall panel. Int. J. Coal Geol. **95**, 20-33 (2012). DOI: https://doi.org/10.1016/j.coal.2012.02.003

[40] S.S. Ahmed, A. Marwan, Y. Gunzburger, V. Renaud, 3D numerical simulation of the goaf due to large-scale longwall mining. International Congress and Exhibition "Sustainable Civil Infrastructures: Innovative Infrastructure Geotechnology" GeoMEast 2017: Numerical Analysis of Nonlinear Coupled Problems pp. 121-131 (2017).

[41] M. Płonka, S. Rajwa, Difficulties observed in operating powered roof support during work in lower range of its working height, Mining – Informatics, Automation and Electrical Engineering. **4** (536), 45-64 (2018). DOI: https://doi.org/10.7494/miag.2018.4.536.45

[42] P. Mao, H. Hashikawa, T. Sasaoka, H. Shimada, Z. Wan, A. Hamanaka, J. Oya, Numerical Investigation of Roof Stability in Longwall Face Developed in Shallow Depth under Weak Geological Conditions. Sustainability **14**, 10-36 (2022). DOI: https://doi.org/10.3390/su14031036

[43] P.M.V. Nguyen, T. Olczak, S. Rajwa, An investigation of longwall failure using 3D numerical modelling – A case study at a copper mine. Studia Geotechnica et Mechanica **43** (4), 389-410 (2021). DOI: https://doi.org/10.2478/sgem-2021-0019

[44] G. Song, Y.P. Chugh, J. Wang, A numerical modelling study of longwall face stability in mining thick coal seams in China. Int. J. Mining and Mineral Engineering **8** (1), 35-55 (2017). DOI: https://doi.org/10.1504/IJMME.2017.082682

[45] S. Rajwa, The Influence of the Geometrical Construction of the Powered Roof Support on the Loss of a Longwall Working Stability Based on the Practical Experience. Archives of Mining Sciences **65** (3), 511-529 (2020). DOI: https://doi.org/10.24425/ams.2020.134132

[46] T. Janoszek, The assessment of longwall working stability based on the Mohr-Coulomb stress criterion – numerical analysis. Archives of Mining Sciences **65** (3), 493-509 (2020). DOI: https://doi.org/10.24425/ams.2020.134131

[47] A.H. Wilson, The stability of underground workings in the soft rocks of the coal measures. Int. J. Min. Eng. **1**, 91-187 (1982). DOI: https://doi.org/10.1007/BF00880785

[48] A.A. Campoli, T.M. Barton, F. Dyke, M. Gauna, Gob and gate road reaction to longwall mining in bump-prone strata (No. 9445). US Department of the Interior, Bureau of Mines, Washington, D.C., USA (1993).

[49] E. Esterhuizen, C. Mark, M.M. Murphy, Numerical model calibration for simulating coal pillars, gob and overburden response. In: Proceedings of the 29th International Conference on Ground Control in Mining, West Virginia, pp 44-57 (2010).

[50] N. Yasitli, B. Ünver, 3D numerical modeling of longwall mining with top-coal caving. International Journal of Rock Mechanics and Mining Sciences **42**, 219-235 (2005). DOI: https://doi.org/10.1016/j.ijrmms.2004.08.007

[51] Q.S. Bai, S.H. Tu, X.G. Zhang, C. Zhang, Y. Yuan, Numerical modeling on brittle failure of coal wall in longwall face – a case study. Arabian Journal of Geosciences **7** (2013). DOI: https://doi.org/10.1007/s12517-013-1181-1